J Mater Sci: Mater Electron (2015) 26:1045–1052
DOI 10.1007/s10854-014-2503-0

Magnetically roll-oriented $LaFeO_3$ nanospheres prepared using oxalic acid precursor method

L. M. Salah · M. M. Rashad · M. Haroun · M. Rasly · M. A. Soliman

Received: 7 August 2014 / Accepted: 10 November 2014 / Published online: 15 November 2014

Abstract Roll-oriented lanthanum orthoferrite $LaFeO_3$ powders have been successfully synthesized using oxalic acid precursor method. Well crystalline $LaFeO_3$ phase was obtained at different annealing temperatures from 600 to 1,000 °C for 2 h. FT-IR spectrum indicated that two active vibrational bands were assigned at 555 and 400 cm^{-1} imputed the formation of lanthanum orthoferrite. The average particle size of $LaFeO_3$ powders were ranged from 50 to 150 nm. The magnetic properties of $LaFeO_3$ samples exhibited a weak ferromagnetic behavior at the room temperature. The shape and surface interface anisotropy were so far strong forming a roll-orientation of particles. The interplay between magnetic properties and annealing temperature showed that the low magnetic interactions between particles were observed as the result of large particles size produced and low surface–interface anisotropy occurred. Hence, microstructures were gradually transformed to tube- and then fibrous-like structures with increasing the annealing temperature. Results are explained in basis of spin–orbit interactions between particles. Furthermore, analysis of the AC electrical data in impedance and dielectric permittivity formalisms revealed the presence of three relaxation processes in $LaFeO_3$, with sufficiently different relaxation times.

L. M. Salah · M. Haroun · M. A. Soliman
Physics Department, Faculty of Science, Cairo University, Giza, Egypt

M. M. Rashad (✉) · M. Rasly
Central Metallurgical Research and Development Institute, P.O. Box 87, Helwan, Cairo, Egypt
e-mail: rashad133@yahoo.com; mrashad@cmrdi.sci.eg

1 Introduction

Admittedly, nanomaterials provide scientists a unique opportunity to develop new properties that are unachievable using bulk sizes [1]. For the current assessment, extensive works have been demonstrated to invest profits of nano size in a multitude of applications. The majority of cases related to the modern chemical industry, are based upon downsizing the mixed metal oxides such as perovskite oxides ABO_3, in which A-site (with ionic radius of >1.0 Å) is a rare-earthmetal and B-site (having ionic radius in the order of 0.6–0.8 Å) is 3d transition metal that remain prominent [2]. Among all perovskite-types, lanthanum orthoferrite, $LaFeO_3$, is the most common compound which has been proposed for several applications such as solid oxide fuel cells [3] catalysts [4], membranes in syngas production [5] chemical sensors [6, 7], water splitting [8] and photocatalytic applications [9].

Monitoring particles morphology "microstructures" is in line with nano-scaling mainstream. The novel phenomena such as non-traditional magnetic, thermal, optical and electrical behaviors could be achieved in materials. For such material shaping can be most likely considered as one-dimensional, not as randomly distributed powders or sintered monolith [10]. Generally, relations between magnetic properties and fiber-like structures of hexagonal ferrite family [11, 12], flower-like structures of hexagonal α-NiS nanoparticles [13], nanocluster-like structures of orthorhombic $LaCrO_3$ powders [14], and one dimensional nanowire-like structure of spinel $NiZnFe_2O_4$ nanoparticles [15] have been studied and new properties are presented. Particularly, many investigations are focused on preparation of nanostructured $LaFeO_3$ using different synthesis methods [16–22]. Nevertheless, controlling microstructures and related physical phenomena have not fully understood yet. Furthermore, long chemical procedures [2] and sometimes

using instrumentations [23] are employed to modify the microstructure. Hence, notions that can simplify preparation and controlling microstructure simultaneously at the nanoscale are considered to be a topic of interest.

The present work thus is the first to (1) present magnetically roll-oriented $LaFeO_3$ nanospheres prepared using the simple organic (oxalic) precursor method, (2) simulate interpretation between magnetic and dielectric properties of $LaFeO_3$ nanoparticles and synthesis annealing conditions and finally (3) postulate a new anomaly for controlling its microstructure at the nanoscale.

2 Experimental

2.1 Materials and procedure

La-orthoferrite $LaFeO_3$ nanospheres have been prepared using the oxalic precursor method. Stoichiometric ratios of lanthanum nitrate $La(NO_3)_3$ and iron nitrate $Fe(NO_3)_3{\cdot}9H_2O$ were dissolved in aqueous solution and then stirred for 15 min on hot plate magnetic stirrer. An appropriate amount of oxalic acid solution was added gradually into the solution. Then, the formed solution was evaporated at 100 °C with constant stirring, resulting in a dried-$LaFeO_3$ oxalate precursor. After that, the precursors were thermally treated for 2 h at different annealing temperatures (600, 800 and 1,000 °C).

2.2 Physical characterization

The phases of the prepared powders were identified from the XRD patterns collected using a Brucker axis D8 diffractometer with Cu K_α ($\lambda = 1.5406$ Å) radiation in 2θ range from 25° to 65°. Fourier transform infrared spectroscopy (FT-IR) was performed at room temperature in transmission mode (Spectrometer JASCO, 6300, Japan) in range 250–650 cm^{-1}. The particle morphology was investigated by field emission scanning electron microscope (FE-SEM, FBI Company, Quanta FEG 250).The magnetic properties of the prepared orthoferrite were carried out at room temperature using a vibrating Sample Magnetometer (VSM, Lake Shore 7410, USA). The dielectric properties were measured using self calibrated Hioki LCR Hi tester type 3531 Z (Japan) at different temperatures from 300 to 850 K and frequencies ranged from 100 kHz to 5 MHz.

3 Result and discussion

3.1 X-ray analysis

Figure 1 shows the XRD patterns of nanocrystalline lanthanum orthoferrites ($LaFeO_3$) samples prepared using oxalic acid precursor method at different annealing temperatures from 400 to 1,000 °C for 2 h. At low annealing temperature 400 °C, the formed powder was completely amorphous. The obtained diffraction profiles of the samples at different annealing temperatures from 600 to 1,000 °C for 2 h were exhibited well-defined single orthorhombic orthoferrite $LaFeO_3$ phase as matched well with JCPDS# 74-2263. Diffraction peaks related to (121), (210), (220), (202), (212), (163), (311), (123) and (242) diffraction planes of $LaFeO_3$ were indexed. However, with increasing the annealing temperature, there are no extra peaks were observed. Moreover, it is clear that all the diffraction peaks have the same fixed position but its sharpness broadness was slightly decreased as the annealing temperature increased. The crystallite sizes of the produced lanthanum ferrite for the most intense peak [(121) plane] were calculated from the XRD data based on the Debye–Scherrer formula. The results indicated that an increase in crystallite size with increasing the annealing temperature was illuminated as a result of crystal growth [12]. Lattice parameters (***a***, ***b*** and ***c***), unit cell volume (V_{cell}) as well as average crystallite size of the orthoferrite specimens are calculated and the results are listed in Table 1. A very fine decrease in both lattice parameters and hence unit cell volume was presented.

3.2 FT-IR spectroscopy

With a view to study the change of normal mode positions and their frequency on annealing temperature of $LaFeO_3$ orthoferrites, FT-IR spectrum data for the respective sites are analyzed and evinced in Fig. 2. The crystal structure of the $LaFeO_3$ is known to be of the distorted GdFeO type

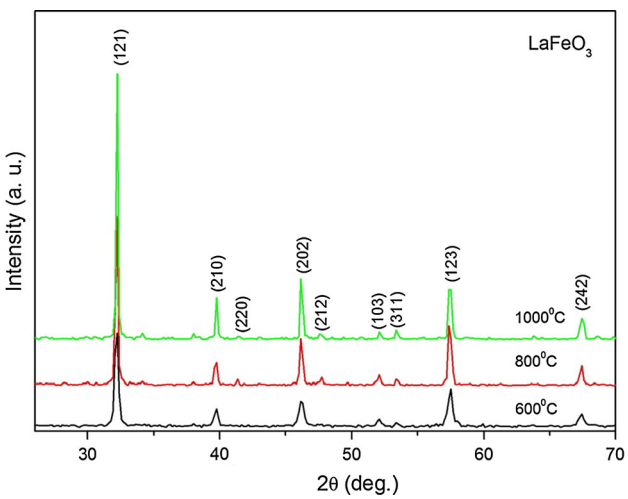

Fig. 1 XRD patterns of $LaFeO_3$ nanospheres prepared using organic acid precursor method at different annealing temperatures (600, 800 and 1,000 °C for 2 h)

Table 1 Structural parameters of $LaFeO_3$ nanospheres prepared using oxalic precursor method at different annealing temperatures (600, 800 and 1,000 °C for 2 h)

Temperature (°C)	Lattice parameters (Å)			Unit cell volume V_{cell} (Å^3)	Crystallite size (nm)
	a	*b*	*c*		
600	5.556	5.552	7.856	242.33	49.6
800	5.554	5.553	7.855	242.26	98.1
1,000	5.551	5.554	7.852	242.08	140.3

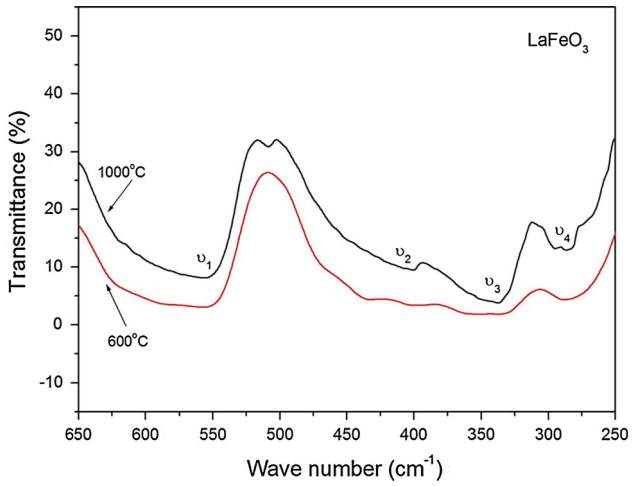

Fig. 2 FT-IR spectra of the produced $LaFeO_3$ nanospheres using organic acid precursor method, annealed at 600 and 1,000 °C for 2 h

structure that a central Fe atom is octahedrally surrounded by its nearest neighbor six O ions. The near-ideal FeO_6 octahedron has the symmetry of the point group, which has six vibrating modes, but only three of them are IR active [20]. The band around 550 cm^{-1} is corresponded to the stretching mode ν_s, which involves the internal motion of a change in length of the Fe–O bond of octahedra. The values around 420 cm^{-1} is assigned to bending mode ν_b of octahedra which is sensitive to a change in the Fe–O–Fe bond angle [24, 25]. The behavior of υ is generally governed by the force constant (K) and mass of the ion (m) forming the bond through the relation $\upsilon \propto \sqrt{\frac{K}{m}}$ [26]. Moreover, it is worth to state that the force constant is inversely proportional to the lattice parameter [27]. It is observed that these three bands remain invariant. This is corresponding well to that analyzed using XRD data. A slight decrease in lattice parameters led to fine increase in force constant and hence vibrational modes along with band positions are shifted to higher wave numbers. Moreover, it can be also vouched from Fig. 2 that the shape effects and the particle size can modify the IR spectrum of ionic powder sample profoundly.

3.3 Morphology

The size and morphology of the synthesized $LaFeO_3$ nanospheres at different annealing temperatures (600, 800 and 1,000 °C for 2 h) were analyzed using FE-SEM images as illustrated in Fig. 3. The results indicated that the particle size increased as increasing annealing temperature; increasing from 50 nm for the annealed-sample at 600 °C to 150 nm for sample annealed at 1,000 °C. These results were in good agreement with that obtained crystallite size data given from XRD analysis based on applying Debye–Scherrer equation. At the same time, polycrystalline particles are not in random orientation state, they are uniformly distributed forming a rolled-like structure. For the image of the smallest particles producing at the lowest annealing temperature 600 °C, it presented the highest degree of well-organized orientation. This type of orientation is originally related to the magnetic interaction forces between particles. This interaction depends strongly on annealing temperature since the particles orientation is decreased with increasing annealing temperature and particles size. With further increasing the annealing temperature up to 800 °C, the particles arrangement was gradually transferred to be a tube-like structure at 800 °C. Finally, it was appeared as a fibrous-like structure at the highest annealing temperature 1,000 °C.

3.4 Magnetic properties

Owing to the slight differences between *M–H* hysteresis loops of La-orthoferrite $LaFeO_3$ samples annealed at 600, 800 and 1,000 °C, it is better to compare only between the highest and the lowest annealed temperature samples. Therefore, Fig. 4 describes the room temperature *M–H* hysteresis loops for $LaFeO_3$ samples, annealed only at 600 and 1,000 °C, whilst the values of magnetic parameters for all investigated samples are given in Table 2.

The results elucidated that ultra-soft characteristic loops were observed for all investigated samples, suggesting that La-orthoferrite $LaFeO_3$ exhibited soft-ferrimagnetic state at the nanoscale whereas it depicted antiferromagnetic state in the bulk form [28]. It is reported that magnetic properties of materials are generally influenced by many factors, such as particles size, structure, surface disorder, morphologies, etc. [12, 29]. A special attention goes the particle size as M_s is increased in correspondence. This affirmed that the actual number of magnetic moments is directly proportional to particles size [30].Furthermore, M_r depends on the magnetic domain rotation which is strongly affected by increasing lattice defects, resulting from increasing the annealing temperature [30]. In spite of increasing M_s and M_r was so inconspicuous, rate of increasing M_r with respect

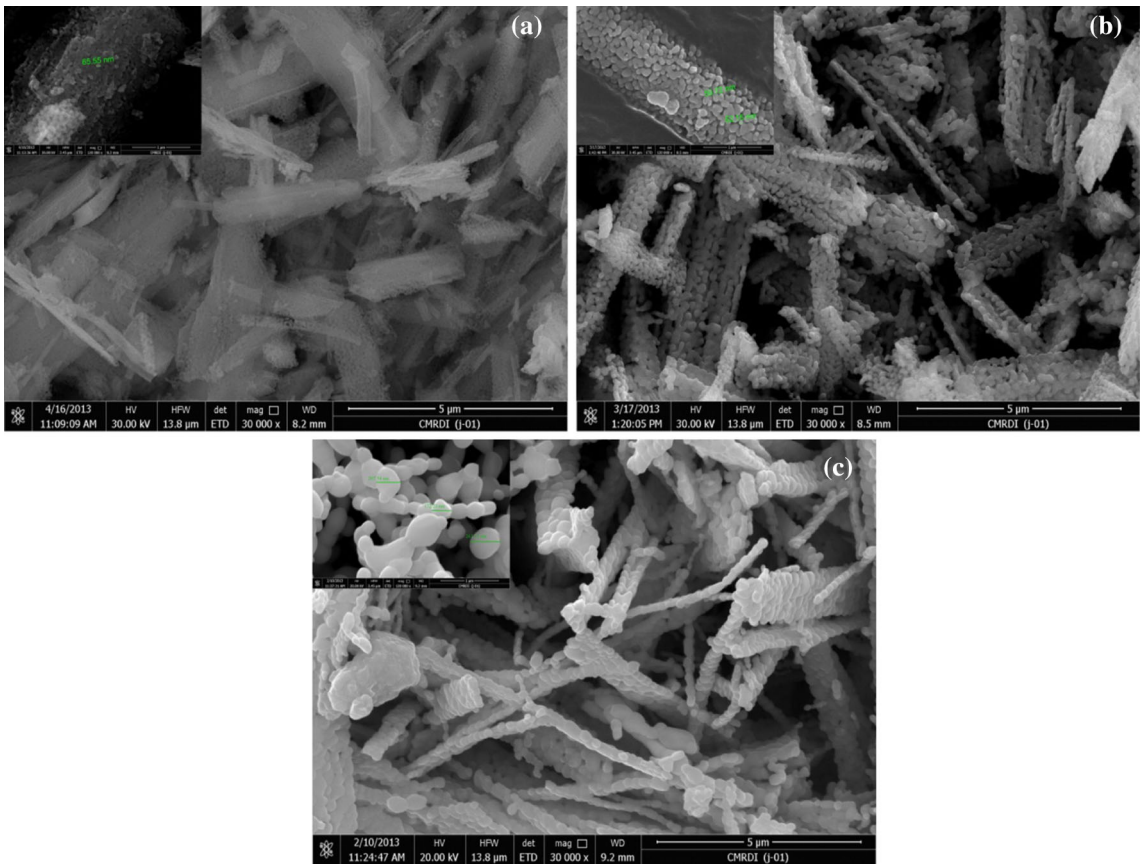

Fig. 3 FE-SEM of the produced $LaFeO_3$ nanospheres using organic precursor method, annealed at **a** 600, **b** 800 and **c** 1,000°C for 2 h

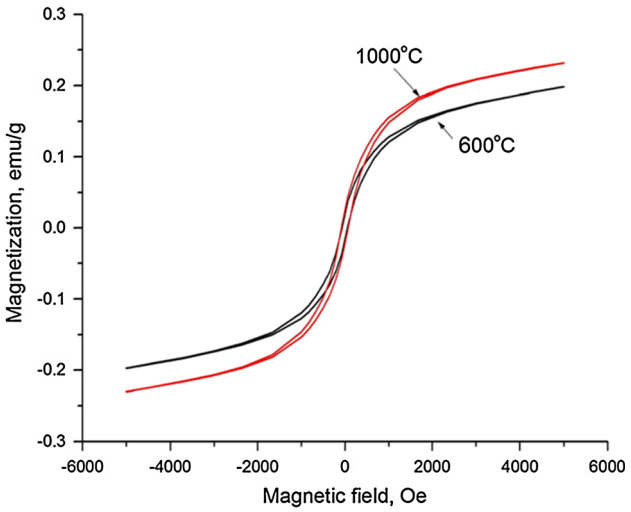

Fig. 4 *M–H* hysteresis loops of the prepared $LaFeO_3$ nanospheres using organic acid precursor method annealed at 600 and 1,000 °C for 2 h

to M_s was smaller and hence squareness ratio was decreased.

A dramatic scenario between both particles morphology and their magnetic properties is simulated for our state of particles. Firstly, at low annealing temperature, 600 °C for 2 h, particles come closed to each other in a well-oriented distribution, forming a strong closed backed rolled-like structure. Increasing temperature to 800 °C for 2 h, particles got larger and their distribution is still homogenously oriented however they are little pet closed to each other, shaping a tube-like structure. At 1,000 °C for 2 h, particles size is so far increased and particles no longer kept the tube-like structure, forming a fibrous-like structure. The second reason that porosity affects the magnetization process because the pore works as a generator of the demagnetization field. The pores tend to hinder the free movement of the magnetic walls during the magnetization process. As a consequence, the intensity of the effective magnetic field applied to the materials is reduced. Increased density reduces the materials s porosity. Therefore, a homogeneous and denser microstructure should favor the flow of the magnetic field through the material, improving its magnetic induction.

Magnetic anisotropy is an intrinsic property describing magnetic materials and is related to the arrangement of atoms in the crystal lattice. This property originates from spin–orbit interactions. However, dealing with the

Table 2 Magnetic properties of the prepared $LaFeO_3$ nanospheres synthesized using oxalic precursor method at different annealing temperatures for 2 h

Magnetic properties				
Annealing temperature (°C)	Saturation magnetization *Ms* (emu/g)	Remanence magnetization *Mr* (emu/g)	Squareness *Mr*/*Ms*	Coercive field Hc (Oe)
600	0.20	0.017	0.10	60
800	0.21	0.019	0.09	73
1,000	0.23	0.023	0.08	80

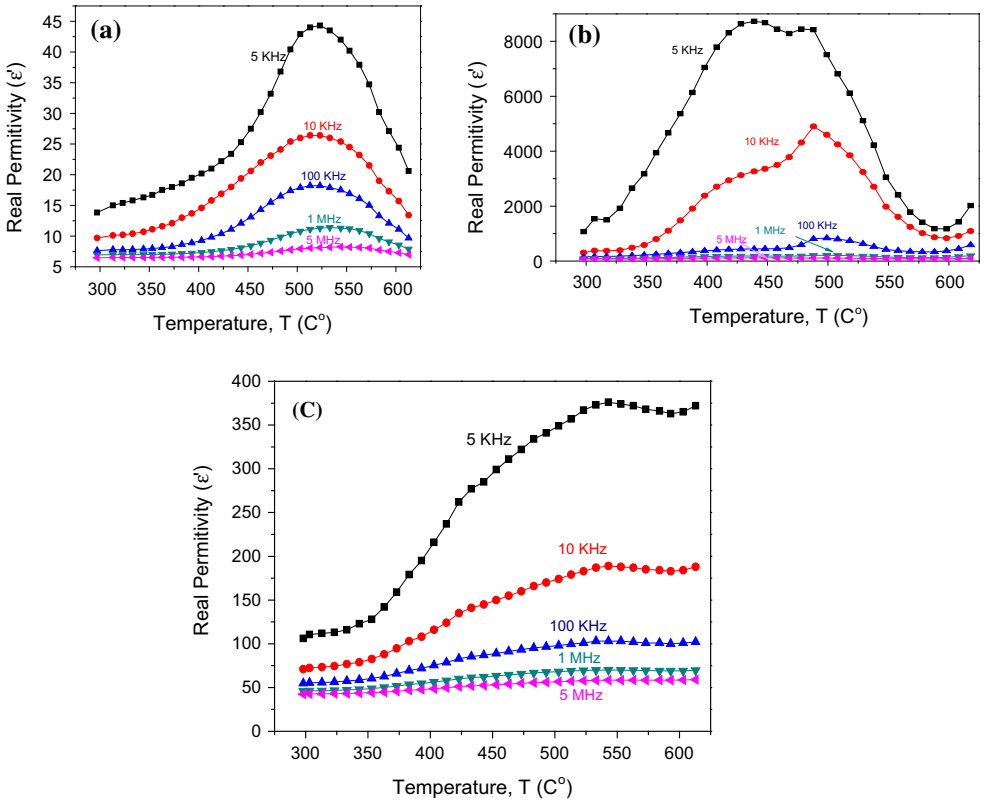

Fig. 5 Complex permittivity dispersion of real part (ε′) for the synthesized $LaFeO_3$ annealed at **a** 600 °C, **b** 800 °C and **c** 1,000 °C for 2 h

randomly oriented particles, it is called induced magneto-crystalline anisotropy. In addition, other parameters should be added to define it such as shape and surface-interface anisotropy [31, 32]. Bruno [33] and Edmonds et al. [34] have expounded that the enhancement in the spin–orbit moment and magneto-crystalline anisotropy were related to the local reduction of symmetry at the surface. As particles size was decreased, the surface area was increased [6], the number of interacted magnetic spins at lattice interface between particles was increased [35] which, in turn, led to increase chance of the spin–orbit interactions between particles. Accordingly, this led to strengthen the shape and surface anisotropy and hence particles strongly attracted to each other. Thus, one could propose the following anomaly: the smaller the particles size, the closer particles presented.

3.5 Dielectric properties

The dielectric properties of orthoferrites are influenced mainly by the preparation method, grain size, and particles morphology. Figure 5a–c displays the temperature dependence of real permittivity (ε′) measured at different frequencies (1 kHz–5 MHz) for annealed samples at 600, 800 and 1,000 °C, respectively. As a normal behavior for all three figures, the value of ε′ is high at low frequency for all the samples and decreases rapidly as the frequency increases and is consistent with combined response of

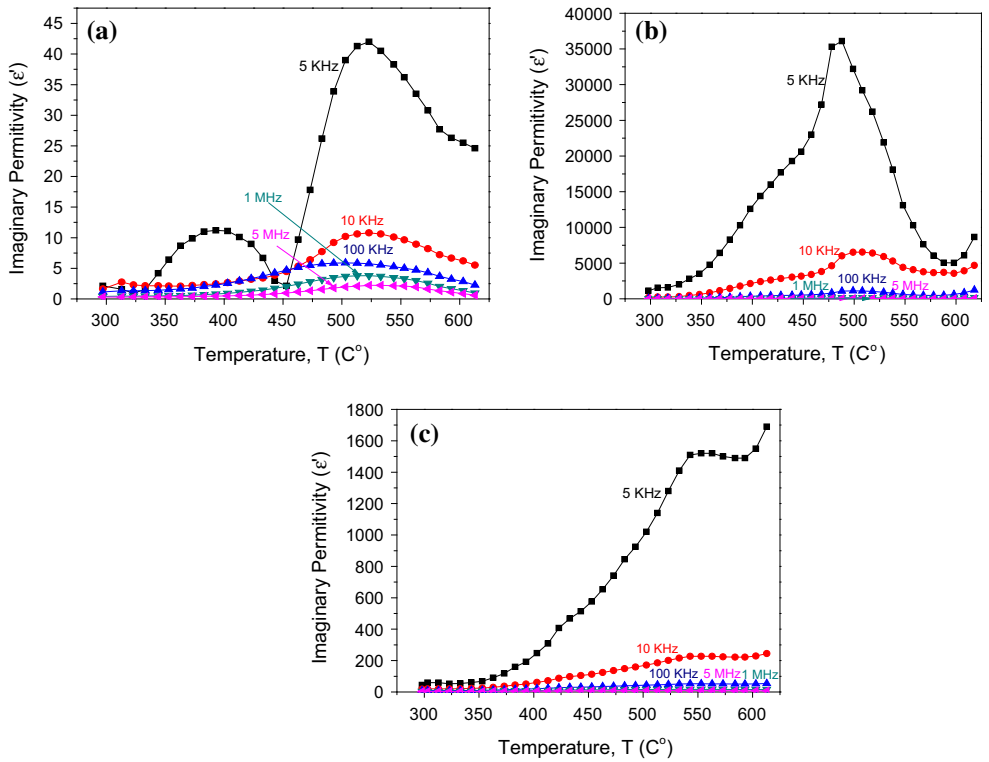

Fig. 6 Complex permittivity dispersion of imaginary part (ε″) for the synthesized $LaFeO_3$ annealed at **a** 600 °C, **b** 800 °C and **c** 1,000 °C for 2 h

orientation relaxation of dipoles and conduction of charge carriers. At higher frequency above 5 MHz, ε′ exhibits a frequency independent behavior. It is also clear that the general trend is the increase in real part of dielectric permittivity (ε′) behavior firstly with increasing temperature up to ∼450 °C. Then, a relaxation process occur, giving raise a peak hump between (450–500 °C) representing to resonance phenomena. After the relaxation process and by increasing the frequency, (ε′) decreases until it reaches a flat region (≤500 °C). In the first frequency, the general increase of (ε′) is due to the increase of the drift mobility of the electrons according to hopping conduction mechanism. The electrons hopping between Fe^{3+} and Fe^{2+} ions present on the octahedral site is thermally activated by increasing the temperature. This hopping causes local displacements in the direction of external electric field. This, in turn, enhances their contribution to the space charge polarization thereby leading to an increase in the value of (ε′) [36]. In the second region, it is describing the relaxation process where the oscillation of ions is equal to that of applied electrical filed. Finally, the electron exchange between Fe^{3+} and Fe^{2+} ions is no longer oscillated in phase in the third region and hence the (ε′) decreased [37]. Moreover, it is observed that the values of ε′ measured at low frequency are larger than that those measured at high frequency. This is due to the fact that the amplitude of vibration of the ions is much greater at the lower frequencies (lower than the natural frequency of vibration of the ions) [38]. A slight difference between three curves of (ε′) could be observed. The increase of the peak is also broadening as increasing annealing temperature. This is due to the intrinsic nature of ferrites "as the annealing temperature increases, as the grains size increases, as the number of grain boundaries decreased". As a consequence, low number of obstacles would prevent oscillations of ions with frequencies alternations. So, the in phase oscillations can stand up to higher frequency, producing more broadening peaks for sample annealed at 1,000 °C comparing to that annealed at 600 and 800 °C [35, 39]. Furthermore, there are two overlapped peaks over the (ε′) curves of annealed sample at 600 °C especially at low frequencies; these peaks could be strongly produced as a result of formation of duplex grain structure [40]. This structure is mostly produced while ferrites mediated with La^{3+} ions especially at low annealing temperature because La^{3+} ions used to immigrate to the particles surface and hence oscillation of electrical dipole moments change from area to another, producing different resonance with applied field [29].

The dependence of the imaginary part of dielectric permittivity (ε″) on frequency at different points of temperature is shown in Fig. 6a–c. Generally, the difference between (ε′) and (ε″) curves could be ascribed in terms of

the presence of maxima at definite frequency through (ε') curves corresponding to minima in (ε'') curves. Each maxima of (ε'') varies from one sample to another as a result of many parameters similarly to those stated in (ε') discussion. From a closer look at the curves, one can find that, the resonance process, which is strongly dependent on the rotational and vibrational motion of localized dipoles, varies with temperature. This means that, the peak position shifts to a lower frequency with increasing temperature, as it appears in Fig. 4c and d as a typical curve. At high frequency, the thermal energy dissipation increases due to increase in friction, leading to an increase in (ε'') [41].

4 Conclusions

In nutshell, the results can be summarized as follows:

- Rolled-like $LaFeO_3$ nanopowders have been successfully synthesized using the simple oxalic precursor method.
- XRD analysis showed that crystallite size of $LaFeO_3$ powders was increased whereas lattice parameters (*a, c*) along with unit cell volume were decreased as increasing annealing temperature. Accordingly, a slight shift to higher wave numbers for vibrational modes was presented through FT-IR spectrum.
- FT-IR spectrum demonstrated that two active vibrational bands were detected at 555 and 400 cm^{-1} as the result of the formation of lanthanum ortho-ferrite.
- The average grain size of the formed $LaFeO_3$ samples was temperature dependent. The grain size was increased from 50 to 150 nm with increasing the annealing temperature from 600 to 1,000 °C for 2 h.
- As annealing temperature increased, M_s and M_r are increased whilst squareness ratio were decreased.
- It was found that the strength of magnetic interface interactions between particles is inversely proportional to particles size: as particles got larger in size, they can't be able to maintain closed packed roll-like structure. So, the structure was gradually transformed to tube- and then fibrous-like structures with increasing the annealing temperature to 800 and 1,000 °C, respectively.
- New anomaly is constructed from the interplay between microstructure and magnetic properties which is the smaller the particles size, the closer particles presented.
- Analysis of the AC electrical data, in impedance and dielectric permittivity formalisms revealed the presence of three relaxation processes in $LaFeO_3$, with sufficiently different relaxation times.
- The observed peaks in imaginary part of dielectric permittivity (ε'') were attributed to a strong correlation between the conduction mechanism and the dielectric behavior exists in ferrites.

Acknowledgments This research is financially supported by the Central Metallurgical Research and Development Institute, Egypt.

References

1. M.L. Lau, H.G. Jiang, R.J. Perez, J. Juarezislas, E.J. Lavernia, Nanostruct. Mater. **7**, 847–856 (1996)
2. R. Abazari, S. Sanati, Superlattices Microstruct. **64**, 148–157 (2013)
3. S. Nakayama, J. Mater. Sci. **36**, 5643–5648 (2001)
4. M.M. Velichkova, T. Lazarova, V. Tumbalev, G. Ivanov, D. Kovacheva, P. Stefanov, A. Naydenov, Chem. Eng. J. **231**, 236–244 (2013)
5. F. He, K. Zhao, Z. Huang, X. Li, G. Wei, H. Li, Chin. J. Catal. **34**, 1242–1249 (2013)
6. J. Zhao, Y. Liu, X. Li, G. Lu, L. You, X. Liang, F. Liu, T. Zhang, Y. Du, Sens. Actuators B **181**, 802–809 (2013)
7. P. Song, Q. Wang, Z. Zhang, Z. Yang, Sens. Actuators B **147**, 248–254 (2010)
8. N.T. Saumitra, V.J. Meenal, S.P. Priyanka, A.M. Priti, S.R. Sadhana, K.L. Nitin, Int. J. Hydrogen Energy **37**, 10451–10455 (2012)
9. S. Thirumalairajan, K. Girija, I. Ganesh, D. Mangalaraj, C. Viswanathan, A. Balamurugan, N. Ponpandian, Chem. Eng. J. **209**, 420–428 (2012)
10. R.C. Pullar, Prog. Mater. Sci. **57**, 1191–1334 (2012)
11. R.C. Pullar, I.K. Bdikin, A.K. Bhattacharya, J. Eur. Ceram. Soc. **32**, 905–913 (2012)
12. M. Rasly, M.M. Rashad, J. Magn. Magn. Mater. **58**, 337–338 (2013)
13. C. Tang, C. Zang, J. Su, D. Zhanga, G. Li, Y. Zhanga, K. Yu, Appl. Surf. Sci. **257**, 3388–3391 (2011)
14. M.M. Rashad, S.M. El-Sheikh, Mater. Res. Bull. **46**, 469–477 (2011)
15. S.M. El-Sheikh, M.M. Rashad, F.A. Harraz, J. Nanopart. Res. **15**, 1967 (2013)
16. H. Zhang, P. Song, D. Han, Q. Wang, Physica E Low Dimens. Syst. Nanostruct. **63**, 21–26 (2014)
17. R. D. Kumar, R. Jayavel, J. Mater. Sci. Mater. Electron. **25**, 3953–3961 (2014). doi:10.1007/s10854-014-2113-x
18. K.M. Parida, K.H. Reddy, S. Martha, D.P. Das, N. Biswa, Int. J. Hydrogen Energy **35**, 12161–12168 (2010)
19. J. Zhao, Y. Liu, X. Li, G. Lu, L. You, X. Liang, F. Liu, T. Zhang, Y. Du, Sens. Actuators B Chem. **181**, 802–809 (2013)
20. Z. Kaiwen, W. Xuehang, W. Wenwei, X. Jun, T. Siqi, L. Sen, Adv. Powder Technol. **24**, 359–363 (2013)
21. P. Tang, Y. Tong, H. Chen, F. Cao, G. Pan, Curr. Appl. Phys. **13**, 340–343 (2013)
22. T. Liu, Y. Xu, Mater. Chem. Phys. **129**, 1047–1050 (2011)
23. W.-Y. Lee, H.J. Yun, J.-W. Yoon, J. Alloys Compd. **583**, 320–324 (2014)
24. X. Wang, Q. Cui, Y. Pan, G. Zou, J. Alloys Compd. **354**, 91–94 (2003)
25. H.C. Gupta, M.K. Singh, L.M. Tiwari, J. Phys. Chem. Solids **64**, 531–533 (2003)
26. A.M. Shaikh, S.A. Jadhav, S.C. Watawe, B.K. Chougule, Mater. Lett. **44**, 192–196 (2000)
27. M.M. Rashad, M. Rasly, H.M. El-Sayed, A.A. Sattar, I.A. Ibrahim, Appl. Phys. A **112**(4), 963–973 (2013)
28. D. Treves, J. Appl. Phys. **36**, 1033–1039 (1965)
29. M.M. Rashad, M. Rasly, H.M. El-Sayed, A.A. Sattar, I.A. Ibrahim, J. Korean Phys. Soc. **63**, 821–825 (2013)
30. M.M. Rashad, H.M. El-Sayed, M. Rasly, M.I. Nasr, J. Magn. Magn. Mater. **324**, 4019–4402 (2012)

31. S.V. Vonsovskii, K.B. Vlasov, J. Exp. Theor. Phys. (USSR) **25**, 327 (1953)
32. M.M. Rashad, M. Bahgat, M. Rasly, S.I. Ahmed, Mater. Sci. Eng. B **178**, 1076–1080 (2013)
33. P. Bruno. Physical origins and theoretical models of magnetic anisotropy, in: *Magnetismus von Festkörpern und grenzflächen*, ed. by P.H. Dederichs, P. Grünberg, W. Zinn. 24 IFF-Ferienkurs, ForschungszentrumJülich P, 24-.& -24.28 (1993)
34. K.W. Edmonds, C. Binns, S.H. Baker, S.C. Thornton, C. Norris, J.B. Goedkoop, M. Finazzi, N.B. Brookes, Phys. Rev. **60**, 472 (1999)
35. M.M. Rashad, H.M. El-Sayed, M. Rasly, A.A. Sattar, I.A. Ibrahim, J. Mater. Sci. Mater. Electron. **24**, 282–289 (2013)
36. K.M. Batoo, S. Kumar, C.G. Lee, Alimuddin, Curr. Appl. Phys. **9**, 1397–1406 (2009)
37. A.M. Abo El Ata, S.M. Attia, T.M. Meaz, Solid State Sci. **6**, 61–69 (2004)
38. M.A. Ahmed, N. Okasha, B. Hussein, J. Alloy. Compd. **553**, 308–315 (2013)
39. M. El-Saadawy, J. Magn. Magn. Mater. **219**, 69–72 (2000)
40. A. Goldman, *Modern Ferrite Technology*, 2nd edn. (Springer, Pittsburgh, 2006)
41. M.A. Ahmed, G. Abd-Ellatif, M. Rashad, J. Magn. Magn. Mater. **232**, 194–204 (2001)